Single gallium nitride nanowire lasers

JUSTIN C. JOHNSON[1], HEON-JIN CHOI[1,2], KELLY P. KNUTSEN[1], RICHARD D. SCHALLER[1], PEIDONG YANG*[1,2] AND RICHARD J. SAYKALLY*[1]

[1]Department of Chemistry, University of California, Berkeley, California 94720-1460, USA
[2]Materials Science Division, Lawrence Berkeley National Laboratory, Berkeley, California 94720, USA
*e-mail: saykally@uclink.berkeley.edu; p_yang@cchem.berkeley.edu

Published online: 15 September 2002; doi: 10.1038/nmat728

There is much current interest in the optical properties of semiconductor nanowires, because the cylindrical geometry and strong two-dimensional confinement of electrons, holes and photons make them particularly attractive as potential building blocks for nanoscale electronics and optoelectronic devices[1,2], including lasers[3,4] and nonlinear optical frequency converters[5]. Gallium nitride (GaN) is a wide-bandgap semiconductor of much practical interest, because it is widely used in electrically pumped ultraviolet–blue light-emitting diodes, lasers and photodetectors[6,7]. Recent progress in microfabrication techniques has allowed stimulated emission to be observed from a variety of GaN microstructures and films[8,9]. Here we report the observation of ultraviolet–blue laser action in single monocrystalline GaN nanowires, using both near-field and far-field optical microscopy to characterize the waveguide mode structure and spectral properties of the radiation at room temperature. The optical microscope images reveal radiation patterns that correlate with axial Fabry–Perot modes ($Q \approx 10^3$) observed in the laser spectrum, which result from the cylindrical cavity geometry of the monocrystalline nanowires. A redshift that is strongly dependent on pump power (45 meV μJ cm^{-2}) supports the idea that the electron–hole plasma mechanism is primarily responsible for the gain at room temperature. This study is a considerable advance towards the realization of electron-injected, nanowire-based ultraviolet–blue coherent light sources.

Stimulated emission from bulk GaN at low temperatures was first reported[10] in the 1970s, to be followed the early 1990s by the achievement of room-temperature lasing in thin films[11]. Lasing thresholds as low as 200 kW cm^{-2} have been achieved in micropillar structures (tens to hundreds of micrometres in diameter, several micrometres thick), with longitudinal whispering gallery modes (WGMs) being the dominant cavity modes[8]. For large diameters (diameter d much greater than the wavelength λ), transverse WGMs are possible, which result from trajectories that traverse a polygonal cross-section near the edges of the cylinder[12,13]. For smaller structures ($d \leq \lambda$) such as those studied here, WGMs have high scattering losses due to diffraction[14], and axial Fabry–Perot waveguide modes (separated by $\Delta\lambda = \lambda^2/[2Ln(\lambda)]$, where $n(\lambda)$ is the dispersion-corrected refractive index and L is the cavity length) are expected to dominate. The nature of the nanowire laser modes can be characterized through near- and far-field optical microscopy, where the distribution and direction of the laser radiation is observed.

The electronic properties of GaN nanowires grown by various methods have been extensively studied[15,16], but the optical emission has not. Figure 1a and b shows typical scanning electron microscopy (SEM) and high-resolution transmission electron microscopy (HRTEM) images of the GaN nanowires studied here. These results establish the highly monocrystalline nature of the GaN nanowires. The wires typically have lengths up to several hundred micrometres and diameters between 30 and 150 nm, although some have diameters approaching 0.5 μm (ref. 17). Figure 1c is an SEM image of an isolated nanowire dispersed on the sapphire substrate.

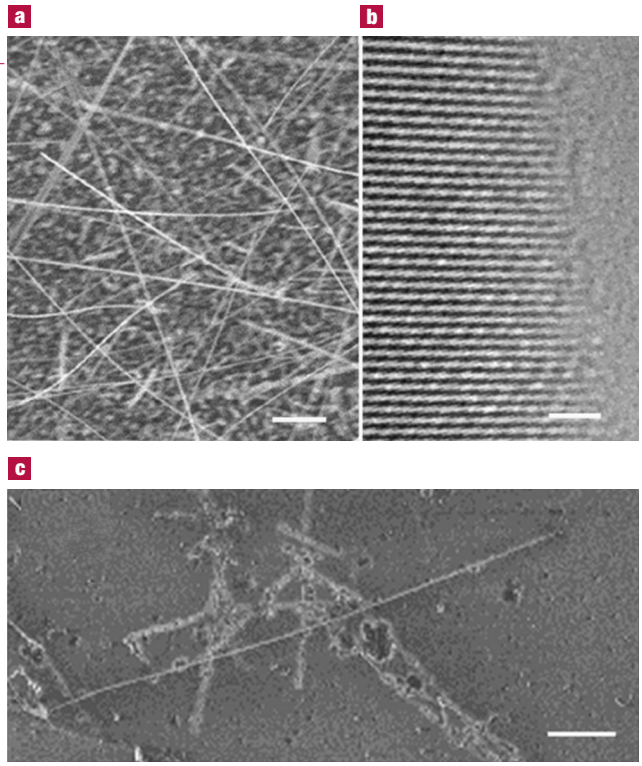

Figure 1 Electron microscopy images of synthesized GaN nanowires. a, Scanning electron microscopy (SEM) images of GaN nanowires grown on sapphire substrate. Scale bar, 3 μm. **b**, High-resolution transmission electron microscopy image of GaN nanowire. Scale bar, 1 nm. **c**, SEM image of single GaN wire after dispersing onto sapphire substrate. Scale bar, 5 μm.

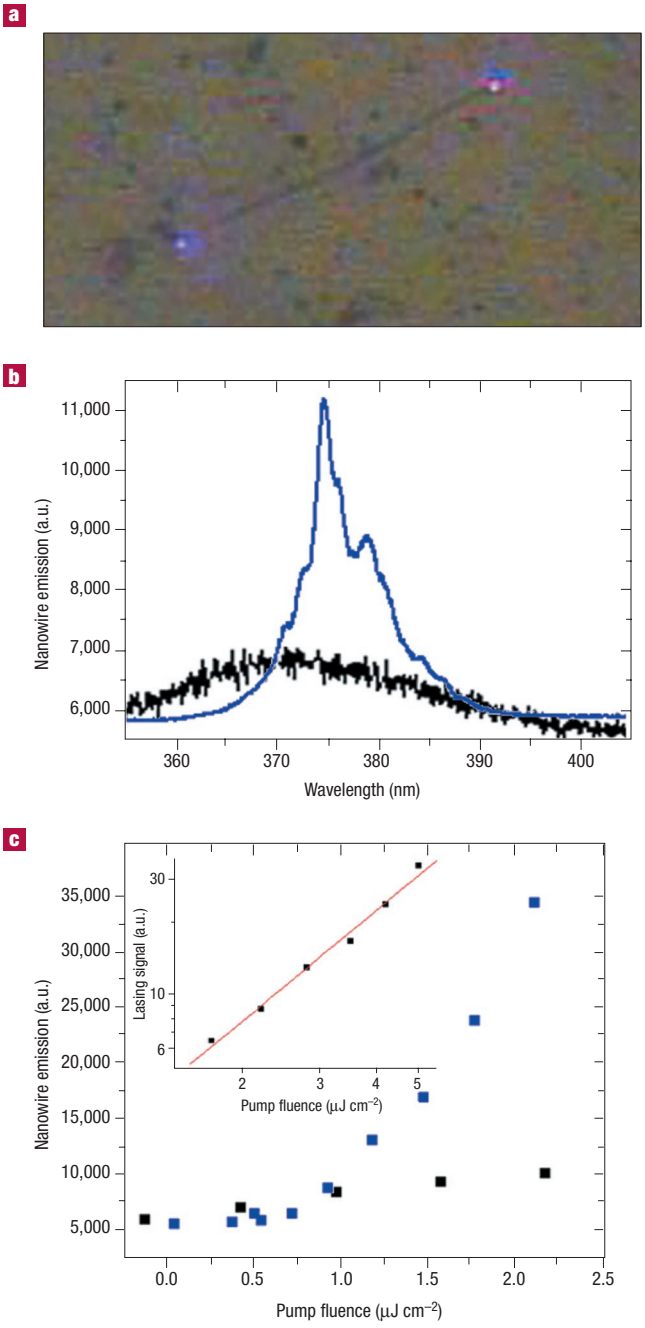

Figure 2 Individual, isolated GaN nanowire laser. a, Far-field image of a single GaN nanolaser (same wire as in Fig. 1c.). The sample was back-illuminated with a lamp to show the structure, and the nanowire was excited with about 3 μJ cm^{-2}. The colour indicates laser emission at the ends of the nanowire. **b**, Spectrum of photoluminescence (black) using 1 mW continuous-wave excitation and lasing (blue) using about 1 μJ cm^{-2} pulsed excitation. **c**, Power dependence of the lasing near threshold (blue) and of photoluminescent emission from a non-lasing region (black). Inset: logarithmic plot of lasing power dependence.

The far-field image in Fig. 2a shows optically pumped (310 nm, 4.0 eV) laser emission from a single, isolated GaN nanowire (diameter ~300 nm, length ~40 μm, as in Fig. 1c). The localization of bright emission at the ends of the wire suggests strong waveguiding behaviour and that the cavity modes are Fabry–Perot (axial) rather than WGMs. Below the lasing threshold, the image has minimal contrast, and the photoluminescence spectrum is broad and featureless (Fig. 2b, black curve). Near the threshold (in this case ~700 nJ cm^{-2}), several sharp (<1.0 nm) features appear in the spectrum, indicating the onset of stimulated emission. Additional laser modes appear as the excitation intensity is increased (Fig. 2b, blue curve). At higher pump fluences, the maximum laser emission was detected at lower energy (>380 nm), indicating a shifting of the gain curve due to bandgap renormalization. This is probably the result of the formation of an electron–hole plasma (EHP), shown to be the dominant lasing mechanism for GaN at high temperatures because of its weakly bound excitons (~25 meV) and coulombic screening at high excitation intensities[18]. This behaviour has been studied in GaN microstructures and thin films; it has been postulated, however, that nanostructures would show enhanced excitonic effects (leading to lower lasing threshold) if the size of the structure approached the exciton Bohr radius (11 nm for GaN)[19].

The dependence of the laser emission on pump fluence is shown in Fig. 2c. Below threshold, the photoluminescence dependence is linear, but a superlinear increase in emission intensity with pump fluence is observed at about 700 nJ cm^{-2}. This is characteristic of stimulated emission, and a log–log plot of the power dependence above threshold shows an approximate quadratic dependence on the pump fluence (inset). The power dependence of photoluminescence from nonlasing GaN material is linear even at high excitation fluence (Fig. 2c, black).

It is difficult to determine a value of the gain coefficient, g, for a single nanowire, because conventional methods for determining g require the length of a sample to be varied with constant cross-section. An estimate of the gain threshold G_{th}, however, can be made from $G_{th} = (2L)^{-1} \ln(R^2)^{-1}$, where L is the length of the gain medium and R is the reflectivity of the end faces[20]. From the refractive indices of air and GaN (1.0 and 2.5, respectively), G_{th} is roughly 400–1,000 cm^{-1}, depending on the length of the nanowire studied. This estimated value lies within the range of those previously reported[20,21]. Using typical values for the absorption coefficient (10^5 cm^{-1}) and the radiative recombination coefficient (1.3×10^{-8} cm^3 s^{-1}), we estimated the electron–hole pair density to be between 5×10^{18} cm^{-3} and 2×10^{19} cm^{-3} for the pump intensities used to study lasing. The Mott density, a measure of the transition from excitons to completely ionized carriers, is estimated to be in the range 5×10^{18} to 1×10^{19} cm^{-3}, indicating that pump fluences near and above threshold create sufficient carrier densities to support EHP behaviour in the GaN nanowires[22].

Figure 3 shows a series of far-field spectra taken as a function of pump fluence on a wire that is 16 μm long and 400 nm in diameter. The spacing of the modes is roughly constant (~1.7 nm), and as many as 12 longitudinal cavity modes are observed at high pump fluence (Fig. 3c). A clear redshift of the gain profile is evident from 400 nJ cm^{-2} to 2,000 nJ cm^{-2}, as shown quantitatively in Fig. 3d (squares). The redshift (about 45 meV μJ cm^{-2}) is initiated above a threshold pump fluence, similar to what is observed in photoluminescence and stimulated emission attributed to EHP[22,23]. The apparent saturation of the redshift is also reproduced in the power dependence (Fig. 3e). This suggests that the redshift is not simply due to sample heating (which might cause a consistently linear shift in the bandgap energy), but is rather due to EHP effects that are proportional to the excited carrier density, which saturates at high excitation intensity. Heating is expected to be minimized by the use of femtosecond pump pulses, and no discernible (<0.1 nm, $\Delta T < 20$ K) redshift is observed for individual modes on this wire. This ΔT sets an upper limit of ~1 nm on the bandgap shift owing to heating, whereas a 5 nm gain-curve shift was actually observed. Shifting of individual modes by up to 0.5 nm was found for smaller-diameter wires (150 nm) at similar

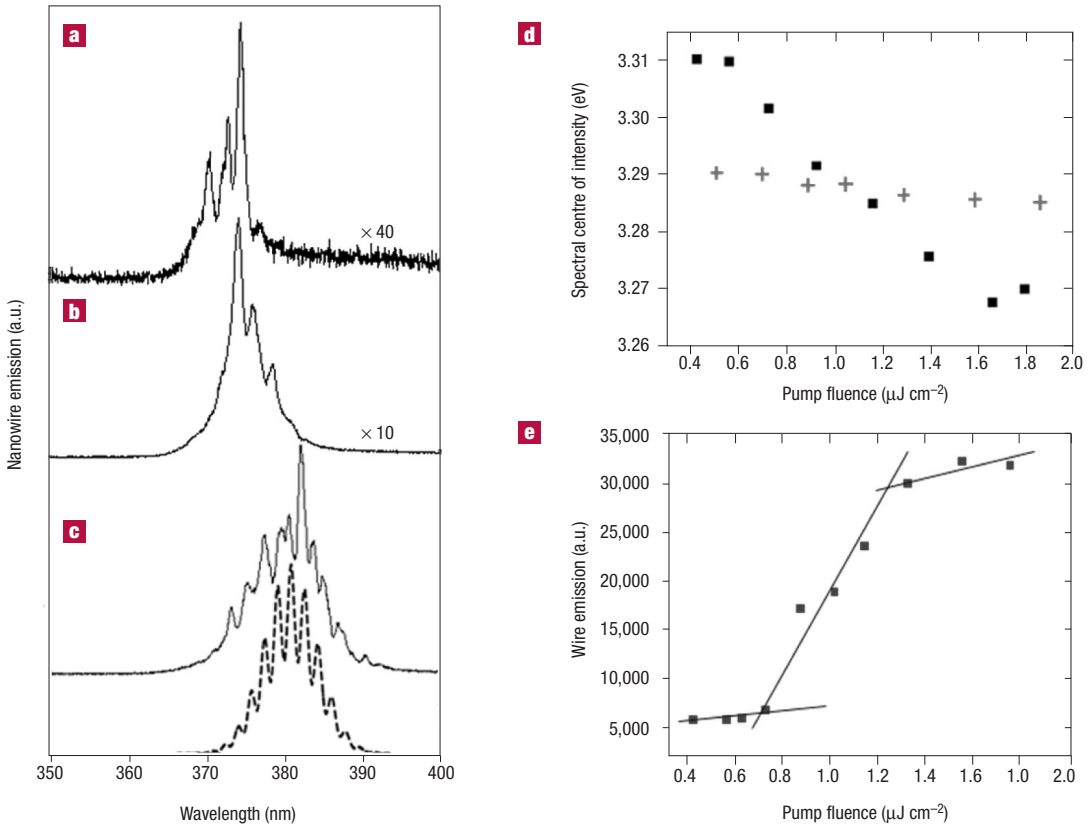

Figure 3 Spectral power dependence of nanolaser emission. a–c, Nanowire laser emission at 0.7, 1.2 and 2 μJ cm^{-2}, respectively. Dashed curve, simulation of nanowire resonator spectral properties, considering equal contributions of one- and two-pass stimulated emission. **d**, Redshift of centre of spectral intensity as a function of pump fluence (squares), calculated by integrating under the spectral emission at each pump fluence. Crosses, redshift of an individual longitudinal cavity mode as a function of pump fluence for a wire of 150 nm diameter, showing the change in the refractive index (and thus effective cavity length). **e**, Overall power dependence of the lasing for a single GaN wire, showing gain pinning. Lines are drawn to indicate the three different emission regimes: spontaneous emission, stimulated emission, and gain-pinning.

pump fluences (Fig. 3d, crosses), indicating a probable temperature change of less than 50 K (ref. 24). It is possible that heating would play a larger role for even smaller nanowires.

A simulation of the nanolaser cavity emission is included below the measured spectrum in Fig. 3c, in which the gain curve and cavity confinement time are considered. Traversing the cavity twice (260 fs) assuming unity gain produces a spectrum with linewidths of 0.6–1.0 nm, consistent with both the experimental data and theory ($\Delta\nu = (2\pi t_c)^{-1}$, where t_c is the cavity confinement time)[25]. The cavity has a low intrinsic finesse (F) because of the low reflectivity (R) of the end faces (~19%) (where $F=\pi R^{1/2}/(1-R)$), dictating that the cavity confinement time will be much shorter than the spontaneous and stimulated emission lifetimes (>100 ps)[26]. The simulation includes an equal contribution of signal from one-pass amplified spontaneous emission (ASE). This could be the source of the observed strong background at high pump fluence, which causes the cavity modes to appear less resolved for some wires. The multi-pass lasing modes are always observed at the lowest threshold, whereas the ASE becomes evident at a higher pump fluence that depends on the particular wire studied. Such ASE has also been observed in other GaN microstructures[8]. The relative amounts of stimulated and spontaneous gain yield an estimate for the average cavity confinement time corresponding to one to three half-passes through the nanowire.

Analysis of the laser linewidth gives a cavity Q factor ($\nu/\Delta\nu = 2\pi\nu t_c$) between 500 and 1,500 for most wires studied. Although this value of Q is much lower than that observed in larger microdisk and microsphere lasers, it is comparable to semiconductor microdisk lasers having subwavelength thicknesses (~0.2 μm). In terms of threshold (<500 nJ cm^{-2} in some cases) and mode volume (<10 cubic wavelengths), these nanolasers are unique active resonators.

To obtain images of the lasing nanowires at higher spatial resolution, we used near-field scanning optical microscopy (NSOM), which provides simultaneous optical and topographical images[27]. The single GaN wire (length ~30 μm, diameter 150 nm) in Fig. 4 shows clear waveguiding and lasing behaviour. Figure 4a shows a combined topographic and ultraviolet–blue photoluminescence image of the bright laser emission confined to the nanowire end. The spatial pattern of this emission is complicated, as is also observed for ZnO nanolasers, suggesting that there is significant intrinsic structure in the nanolaser beam in the near field[28], or that additional scattering is occurring as the light leaves the end faces. In some cases, weaker laser emission was detected in regions other than the

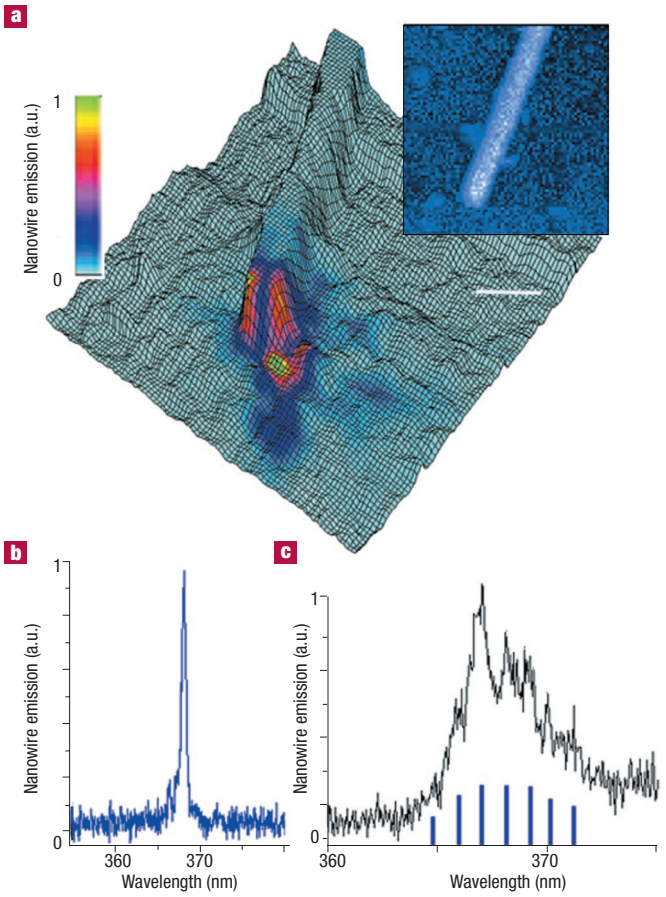

Figure 4 Near-field microscopy of single GaN nanolaser. a, Combined topographic and optical image of the tip of a single GaN nanowire (30 μm long, 150 nm diameter). Scale bar, 1 μm. Inset: shear-force feedback image of nanowire. **b**, Near-field spectrum from just beyond the nanowire end. **c**, Far-field spectrum from the wire showing longitudinal cavity modes (denoted by sticks below spectrum) appearing near the lasing threshold.

ends of the nanowire, suggesting that there are small defects or fractures in some wires caused during sample preparation.

The near-field optical spectrum shown in Fig. 4b was taken just beyond the end of the nanowire tip in the bright emission region. An almost flat background accompanies the single lasing peak (~0.8 nm linewidth) in this case, indicative of the high directionality of the nanolaser radiation (because the spatial selectivity of the probe rejects any unguided photoluminescence). A far-field spectrum (Fig. 4c) very near threshold shows a much broader overall feature (>5 nm), apparently because of additional photoluminescent background and multiple cavity modes collected from the entire wire. The modes are spaced at about 1.0 nm, in good agreement with expected spacing of longitudinal Fabry–Perot modes. These modes are difficult to discern because the mode spacing is similar to the lasing linewidth, which is especially apparent at higher pump fluences, where the emission broadens and shifts to longer wavelength.

In terms of pump fluence, the measured thresholds P_t for the GaN nanowire waveguide resonators are slightly higher than observed in zinc oxide nanowires that lase through excitonic recombination, although they are lower than those reported for other types of GaN microstructures, which may be due to the reduction in mode volume ($P_t \propto V_m$)[29]. The power dependence of the spectral emission suggests that the EHP mechanism is responsible for the optical gain in the GaN wires, which is consistent with previous experimental and theoretical studies. The aspect ratio of these nanolasers (>250:1) is significantly larger than observed for ZnO nanolasers, and theoretically, lasing could be observed in smaller-diameter wires (<70 nm), although coupling of photoluminescence into lasing modes instead of radiation modes is expected to decrease with $d < \lambda$, owing to intrinsic diffraction effects. Future experiments will address nanowire lasing near this limit. Coupling these studies with improvements in carrier-injection in nanowires should generate exciting advances in the production of nanoscale photonic and optoelectronic devices.

METHODS

NANOWIRE SYNTHESIS

GaN nanowires were synthesized using a nickel catalyst deposited on sapphire substrate through direct reaction of the gallium metal and ammonia at 900 °C. The nanowires have catalyst particles on their ends, which indicates the vapour–liquid–solid mechanism for growth. X-ray diffraction was used to confirm that the nanowires have the wurtzite crystal structure. To be imaged with the NSOM, the wires were removed from the sapphire substrate by sonication and dispersed onto a sapphire substrate by drop-casting a mixture of ethanol and nanowires. Although they were not studied in detail, wires not broken from the substrate did not show significantly different emission properties.

LASER EXCITATION

The excitation source consists of the fourth harmonic of the signal beam from an optical parametric amplifier (OPA). The pump laser for the OPA is a regeneratively amplified Ti:sapphire oscillator. The OPA signal wavelength is continuously tunable from 1,170 to 1,600 nm, allowing for a frequency-quadrupled beam from 290 to 400 nm, with an average power of 5–10 mW. The ultraviolet pulses are approximately 100–200 fs in duration, with a repetition rate of 1 kHz. The typical pulse energy used for the lasing studies was 50–500 pJ. The laser was directed obliquely to the microscope and focused to an elliptical spot, which was kept relatively large (150 μm by 250 μm) to aid in even illumination of longer wires. A continuous-wave He–Cd laser at 325 nm was used for additional photoluminescence studies.

MICROSCOPY

A microscope objective (NA 0.7) was used for far-field images, which were recorded with a digital video camera. Spectra were collected by coupling the photoluminescence to an optical fibre which was directed to a 0.3-m spectrograph and a charge-coupled device (CCD) cooled in liquid nitrogen (1,340 × 100 pixels, Roper Scientific). The resolution of the spectrograph is about 0.1 nm. The near-field microscope uses a chemically etched silica fibre-optic probe (having a tip diameter of about 100 nm) on a quartz tuning fork in a shear-force feedback scanning mechanism. Simultaneous optical and topographic images are obtained (200 × 200 pixels) by monitoring the feedback signal (which maintains the tip at a constant distance, 5–10 nm, from the sample) and by collecting emission with the single-mode optical fibre (typical collection efficiency 10^{-4}–10^{-5}), which is directed to a photomultiplier tube.

Received 6 July 2002; accepted 24 August 2002; published 15 September 2002.

References

1. Duan, X., Huang, Y., Cui, Y., Wang, J. & Lieber, C. M. Indium phosphide nanowires as building blocks for nanoscale electronic and optoelectronic devices. *Nature* **409,** 66–69 (2001).
2. Wang, J., Gudiksen, M. S., Duan, X., Cui, Y. & Lieber, C. M. Highly polarised photoluminescence and photodetection from single indium phosphide nanowires. *Science* **293,** 1455–1457 (2001).
3. Huang, M. H. *et al.* Room-temperature ultraviolet nanowire nanolasers. *Science* **292,** 1897–1899 (2001).
4. Johnson, J. C. *et al.* Single nanowire lasers. *J. Phys. Chem. B* **105,** 11387–11390 (2001).
5. Johnson, J. C. *et al.* Nonlinear optical mixing in single zinc oxide nanowires. *Nano Lett.* **2,** 279–283 (2002).
6. Morkoc, H. *et al.* Large band-gap SiC, III-V Nitride, and II-VI ZnSe-based semiconductor device technologies. *J. Appl. Phys.* **76,** 1363–1398 (1994).
7. Nakamura, S., Senoh, M. & Mukai, T. High-power InGaN/GaN double-heterostructure violet light emitting diodes. *Appl. Phys. Lett.* **62,** 2390–2392 (1993).
8. Chang, S., Rex, N. B., Chang, R. K., Chong, G. & Guido, L. J. Stimulated emission and lasing in whispering-gallery modes of GaN microdisk cavities. *Appl. Phys. Lett.* **75,** 166–168 (1999).
9. Yang, X. H., Schmidt, T. J., Shan, W. & Song, J. J. Above room temperature near ultraviolet lasing from an optically pumped GaN film grown on sapphire. *Appl. Phys. Lett.* **66,** 1–3 (1995).
10. Dingle, R., Zetterstrom, R. B., Shaklee, K. L. & Leheny, R. F. Stimulated emission and laser action in gallium nitride. *Appl. Phys. Lett.* **19,** 5–7 (1971).
11. Asif Khan, M., Olson, D. T., Van Hove, J. M. & Kuznia, J. N. Stimulated emission from photopumped GaN films. *Appl. Phys. Lett.* **58,** 1515–1517 (1991).
12. Campillo, A. J. & Chang, R. K. in *Optical Processes in Microcavities* Ch. 5 (eds Campillo, A. J. & Chang, R. K.) 167–208 (World Scientific, Singapore, 1996).
13. Chylek, P. Resonance structure of Mie scattering: distance between resonances. *J. Opt. Soc. Am. A* **1,** 822–830 (1984).
14. Gerard, J. M. *et al.* Quantum boxes as active probes for photonic microstructrues: the pillar microcavity case. *Appl. Phys. Lett.* **69,** 449–451 (1996).
15. Duan, X. & Lieber, C. M. Laser-assisted catalytic growth of single crystal GaN nanowires. *J. Am. Chem. Soc.* **122,** 188–189 (2000).

16. Han, W., Fan, S., Li, Q. & Hu, Y. Synthesis of gallium nitride nanorods through a carbon nanotube-confined reaction. *Science* **277,** 1287–1289 (1997).
17. Huang, M. H. *et al.* Catalytic growth of zinc oxide nanowires by vapor transport. *Adv. Mater.* **13,** 113–116 (2001).
18. Bidnyk, S., Schmidt, T. J., Little, B. D. & Song, J. J. Near-threshold gain mechanisms in GaN thin films in the temperature range of 20–700K. *Appl. Phys. Lett.* **74,** 1–3 (1999).
19. Preschilla, N. A. *et al.* Nanocrystalline gallium nitride thin films. *Appl. Phys. Lett.* **77,** 1861–1863 (2000).
20. Domen, K., Kondo, K., Kuramata, A. & Tanahashi, T. Gain analysis for surface emission by optical pumping of wurtzite GaN. *Appl. Phys. Lett.* **69,** 94–96 (1996).
21. Binet, F. *et al.* Realization and optical characterization of etched mirror facets in GaN cavities. *Appl. Phys. Lett.* **72,** 960–962 (1998).
22. Binet, F., Duboz, J. Y., Off, J. & Scholz, F. High-excitation photoluminescence in GaN: Hot-carrier effects and the Mott transition. *Phys. Rev. B* **60,** 4715–4722 (1999).
23. Bagnall, D. M. *et al.* Optically-pumped lasing of ZnO at room temperature. *Appl. Phys. Lett.* **70,** 2230–2232 (1997).
24. Edjer, E. Refractive index of GaN. *Phys. Status Solidi A.* **6,** 445–448 (1971).
25. Svelto, O. *Principles of Lasers* 168 (Plenum, New York, 1998).
26. Jursenas, S. *et al.* Decay of stimulated and spontaneous emission in highly excited homoepitaxial GaN. *Appl. Phys. Lett.* **78,** 3776–3779 (2001).
27. Schaller, R. D. *et al.* Nonlinear chemical imaging nanomicroscopy: From second and third harmonic generation to multiplex (broad-bandwidth) sum frequency generation near-field scanning optical microscopy. *J. Phys. Chem. B* **106,** 5143–5154 (2002).
28. Gmachl, C. *et al.* High power directional emission from microlasers with chaotic resonators. *Science* **280,** 1556–1564 (1998).
29. Slusher, R. E. & Mohideen, U. In *Optical Processes in Microcavities* Ch. 9 (eds Campillo, A. J. & Chang, R.) 315–338 (World Scientific, Singapore, 1996).

Acknowledgements

J.C.J., K.P.K., R.D.S. and R.J.S. are supported by the Physical Sciences Division of the National Science Foundation. H.C. and P.Y. are supported by the Camille and Henry Dreyfus Foundation, 3M Corporation, Beckman Foundation, the National Science Foundation and the University of California, Berkeley. P.Y. is an Alfred P. Sloan Research Fellow. Work at the Lawrence Berkeley National Laboratory was supported by the Office of Science, Basic Energy Sciences, Division of Materials Science of the US Department of Energy. We thank the National Center for Electron Microscopy for the use of their facilities.
Correspondence and requests for materials should be addressed to R.J.S or P.Y.

Competing financial interests

The authors declare that they have no competing financial interests.